Journal of Cardiovascular Magnetic Resonance (2007) **9,** 633–644

ISSN: 1097-6647 print / 1532-429X online
DOI: 10.1080/10976640601093661

informa
healthcare

First-Pass Myocardial Perfusion Cardiovascular Magnetic Resonance at 3 Tesla

Mao-Yuan M. Su, MS,[1,5] Kai-Chien Yang, MD,[2] Chau-Chung Wu, MD, PhD,[2] Yen-Wen Wu, MD,[3] Hsi-Yu Yu, MD,[4] Rung-Yu Tseng, BS,[6] and **Wen-Yih I. Tseng, MD, PhD[5,6]**

Institute of Biomedical Engineering, National Yang-Ming University, Taipei, Taiwan;[1] Department of Internal Medicine,[2] Department of Nuclear Medicine,[3] Department of Surgery,[4] Department of Medical Imaging,[5] National Taiwan University Hospital, Taipei, Taiwan; and Center for Optoelectronic Biomedicine, College of Medicine, National Taiwan University, Taipei, Taiwan[6]

ABSTRACT

Purpose: **To test the feasibility of first-pass contrast-enhanced myocardial perfusion imaging at 3 Tesla and to evaluate the change in perfusion index between normal, remote and ischemic myocardium, we obtained perfusion index from healthy subjects and patients with coronary artery stenosis.** ***Materials and Methods*****: First-pass contrast-enhanced perfusion imaging was performed on 12 patients and 32 age-matched healthy subjects in both rest and dipyridamole-induced stress states. After bolus injection of contrast agent, Gd-DTPA with dose of 0.025 mmol/kg body weight and injection time of 1.5 s, three short-axis images from apex to base of the left ventricle (LV) were acquired for 80 cardiac cycles using saturation recovery turbo FLASH sequence. The maximal upslope (Upslope) was derived from the signal-time curves of the LV cavity and myocardium to measure myocardial perfusion. Within 72 hours after cardiovascular magnetic resonance examination, patients received coronary angiography, and the results were correlated with cardiovascular magnetic resonance results.** ***Results*****: Using our protocol of contrast agent administration, sufficient perfusion contrast was obtained without susceptibility-induced signal drop-out at the interface between LV cavity and the myocardium. In healthy volunteers, Upslope showed no dependence on myocardial segments or coronary territories. Upslope increased significantly from rest to stress in normal myocardium (0.09 ± 0.03 vs. 0.16 ± 0.05, $p < 0.001$) and remote myocardium (0.09 ± 0.03 vs. 0.13 ± 0.03, $p < 0.001$), whereas in ischemic myocardium the change was insignificant (0.11 ± 0.03 vs. 0.10 ± 0.04, $p =$ ns). This resulted in significant difference in the ratio of Upslope at stress to that at rest, representing myocardial perfusion reserve, between ischemic and non-ischemic myocardium (0.96 ± 0.41 vs. 1.71 ± 0.42, $p < 0.001$ for ischemic vs. normal myocardium; 0.96 ± 0.41 vs. 1.59 ± 0.40, $p < 0.001$ for ischemic vs. remote myocardium).** ***Conclusions*****: First-pass gadolinium-enhanced myocardial perfusion imaging at 3 Tesla is feasible. The Upslope ratio can differentiate ischemic from non-ischemic myocardium.**

Received 19 May 2006; accepted 4 October 2006.
Keywords: Myocardial perfusion, 3 Tesla, ischemic heart disease.
The work was originated from the Center for Optoelectronic Biomedicine, College of Medicine, National Taiwan University, 1 Jen-Ai Road, Section 1, Taipei, Taiwan 10016. The study was supported in part by the National Taiwan University Hospital, grant #9261700810, the Grant for Academic Excellence #A-91-FA01-2-4, Ministry of Education, Taiwan, and the National Science Council, R.O.C., grant NSC 94-2614-E-002-002. The authors are indebted to Dr. Gerhab Laub and Mr. Wyncent Wong for their help in installing cardiac protocols on the 3T MR system, and to Mr. Ying-Ding Li and Ruey-Ming Hwang for their assistance in scanning patients.
Correspondence to:
Wen-Yih I. Tseng, MD, PhD
Center for Optoelectronic Biomedicine
College of Medicine
National Taiwan University
1 Jen-Ai Road, Section 1
Taipei
Taiwan 10016
tel: 886-2-2312-345,6 ext. 8758; fax: 886-2-2392-6922
email: wytseng@ntumc.org

INTRODUCTION

Recent advance in fast cardiovascular (CMR) techniques allows assessment of myocardial perfusion by exploring time-resolved dynamic enhancement of the heart during the first pass of contrast medium (CM). This MR-based measurement has been considered a potential tool to assess myocardial perfusion owing to its excellent spatial resolution, high perfusion contrast and absence of ionizing radiation (1). The original data from Gould (2) showed that the maximum coronary blood flow and the coronary flow reserve are more sensitive to detection of coronary stenosis than resting blood flow. CMR can be used to extract semiquantitatively or quantitatively measures of myocardial perfusion, which can be used in analogy to flow measurements for the detection of stenosis. By comparing myocardial perfusion between rest and induced vasodilation state (stress), ischemic myocardium demonstrates blunt hyperemic response due to poor reserve for vasodilation under pharmacological or exercise induction. Many studies have reported that MPR derived from perfusion CMR in combination with pharmacological stress test is sensitive to perfusion impairment in ischemic myocardium (3–7).

Evaluating myocardial perfusion using MR system at 3 Tesla (3T) is potentially advantageous owing to high signal-to-noise ratio (SNR) and perfusion contrast (8–10). However, image degradation due to magnetic susceptibility becomes worse as static magnetic field increases, offsetting the advantages of 3T (11). Clinical protocols of cardiovascular MR at 3T, including effective correction for susceptibility-induced artifact, are currently under active investigation, but reports on the assessment of myocardial perfusion using 3T systems are not available yet. To investigate the feasibility of myocardial perfusion imaging at 3T, this paper aims to determine the optimal protocol of contrast administration, image quality, reproducibility and ability of MPR to differentiate ischemic from non-ischemic myocardium.

MATERIALS AND METHODS

Study Population

Thirty-two volunteers without history of cardiac disease (19 male; age, 49.7 ± 5.0 years) and 12 consecutive patients who presented with symptoms of chest pain (8 male; age, 56.3 ± 15.2 years; p = ns) were recruited in the study. All control subjects, before entering the study, received resting ECG and showed no ECG abnormality. Patients who were found to have cardiac arrhythmias, previous history of revascularization or myocardial infarction were excluded from the study. Detailed clinical information about the patient group is given in Table 1. Subjects reviewed and signed informed consent upon entering the study protocol. The study was carried out under the approval of the Institutional Review Board of our hospital.

Cardiovascular Magnetic Resonance

All subjects were examined in supine position in a 3T MRI scanner (Trio, Siemens, Erlangen, Germany), and an 8-channel cardiac phased-array coil was used for signal reception. Scout images in two and four chamber views were acquired to determine the long axis of the left ventricle (LV), according to which three short-axis planes were localized. The middle plane was located at the mid point of the LV long axis, and the two adjacent planes were separated from the middle plane by one third of the axis length. Perfusion images were acquired in the prescribed short-axis planes, using an ECG-gated non-slice-selective 90° saturation-recovery preparation turbo fast low angle shot (TurboFLASH) pulse sequence, TI = 90 ms; TR/TE/flip angle = 1.08 ms/0.98 ms/10°; bandwidth = 870 Hz/pixel; slice thickness = 8 mm; matrix size = 192 × 144, field of view (FOV) = 400 mm × 240 ~ 300 mm; in-plane resolution = 2.08 mm × 1.67 ~ 2.08 mm, and temporal resolution (data acquisition time per slice) = 160 ms. Parallel imaging was not used in this study. Image acquisition was triggered prospectively by electrocardiographic (ECG) R waves. During each cardiac cycle, three short-axis images were consecutively acquired from apex to base. The acquisition lasted for 80 heart beats, yielding 80 time frames for each level at temporal resolution of one R-to-R interval. Immediately after the initial three scans, a bolus of T1 CM (gadopentetate dimeglumine; 0.025 mmol/kg body weight of dose [Magnevist, Berlex Laboratories, Wayne, NJ, USA]) was injected via left antecubital vein with an injection rate adjusted to keep the injection time at 1.5 s, followed by saline chase of 15 mL. As described in the next paragraph, 0.025 mmol/kg body weight of dose was used based on our optimization study in other seven healthy volunteers in the same 3T system. To reduce respiratory motion, patients were coached to hold their breath when injection began and resumed free breathing whenever they could not hold the breath. The stress study was carried out after the rest study. A dose of 0.14 mg/kg/min of dipyridamole was infused intravenously via right antecubital vein for 4 minutes, and the

Table 1. Clinical data of patients (N = 12)

Patient (Gender/ Age [y])	Clinical Assessment	Luminal Narrowing (>75%) by Conventional Coronary Angiography			EF (%)
		LAD	RCA	LCX	
M/37	Chest tightness				77
M/33	Typical angina	+			76
F/76	Severe palpitation after exercise		+		83
M/54	Typical angina			+	72
M/62	Dyspnea and chest pain				78
M/57	Typical angina				75
F/76	Typical angina	+	+	+	47
M/40	Chest tightness				69
M/59	Typical angina	+	+	+	76
M/71	Typical angina	+			72
F/67	Chest pain				80
M/44	Atypical angina				76

LAD = left anterior descending artery, RCA = right coronary artery, LCX = left circumflex coronary artery. The degree of luminal narrowing was determined by visual inspection of the conventional coronary angiogram with standard criteria. EF (ejection fraction) was assessed by cardiac cine MR imaging.

perfusion imaging began at the 7th minute when the maximal vasodilation was achieved (12). The time interval between rest and stress test was at least 7 minutes. Blood pressure and heart rate were monitored at the first minute (before dipyridamole infusion), 4th minute (right after dipyridamole infusion) and 7th minute (right before the stress study). An antidote, aminophylline, 125 mg of dose, was given intravenously immediately after the stress study.

To assess the myocardial viability, late gadolinium enhancement (LGE) CMR was performed after the perfusion study. We infused the rest of the contrast agent after the stress study and performed the LGE study 10 minutes after the infusion. The total dosage of contrast agent given to a subject was 0.2 mmol/kg body weight. An inversion-recovery prepared segmented turboFLASH sequence, TR/TE/flip angle = 1.6 ms/1.52 ms/20°, FOV = 240 × 350 mm, matrix size = 205 × 256 was acquired on short-axis planes from base to apex at 7 mm slice thickness and 3 mm gap distance. The inversion time was adjusted constantly to null the normal myocardium and was typically in the range of 200 ∼ 300 ms.

Optimization of contrast agent dose

To determine the optimum dose of CM, 6 healthy volunteers received first-pass gadolinium-enhanced CMR. Five different CM doses, 0.0125, 0.025, 0.05, 0.075 and 0.1 mmol/kg body weight, were administered with bolus injection via left antecubital vein. Each subject completed 5 series of data acquisition for 5 different doses in one study session. To avoid dose accumulation, neighboring data acquisitions were separated 30 minutes apart to ensure clearance of CM from the blood. To ensure CM doses were injected within the same time interval, the injection time of the study protocol was fixed at 1.5 s, resulting in different injection rates ranging from 0.83 to 6.6 mL/sec. In each data set, first-pass signal time curves in the LV cavity and myocardium were measured, contrast-enhancement (CE), signal-to-noise ratio (SNR) and contrast-to-noise ratio (CNR) were determined from individual curves. CE was defined as the peak SI subtracted by the baseline SI of the signal-time curve:

$$\text{CE} = \text{peak SI} - \text{baseline SI}. \quad [1]$$

SNR was defined as the peak SI divided by the standard deviation (STD) of the background noise (13):

$$\text{SNR} = \frac{\text{peak SI}}{\text{STD of background Noise}}. \quad [2]$$

CNR was defined as the CE divided by STD of the baseline SI (14):

$$\text{CNR} = \frac{\text{CE}}{\text{STD of baseline SI}}. \quad [3]$$

Coronary angiography

All patients received coronary angiography within 72 hours after the CMR examination. More than 75% reduction of the luminal diameter in major epicardial coronary arteries or their major branches (>2.5 mm in diameter) detected by the angiography was considered hemodynamically-significant stenosis (15). The angiographic results were classified as 1, 2, or 3 vessel disease or negative finding (no significant coronary stenosis). These results were used as reference standard to compare with the results obtained from CMR.

Image data analysis

Image analysis started with alignment of the perfusion images followed by segmentation of the LV cavity and myocardium (16). The LV myocardium at three short-axis levels was divided into 16 equiangular segments, not including apical cap, according to the guidelines provided by the American Heart Association and the American College of Cardiology (17). The baseline SI value for each segment was determined from the first 5–10 images before arrival of the contrast agent to the LV cavity and was used to correct for the depth-dependent signal variation due to the surface coil (14). The mean SI of each segment and in the LV cavity at each time frame was then subtracted by the baseline SI before contrast arrival (Fig. 1). Gamma-variate function (18, 19) was used to smooth-fit the corrected SI data within the time window of the first pass in each segment (Fig. 2). A time window of the first pass was determined from the SI curve of the LV cavity; the time of the onset of contrast arrival and the time of the onset of recirculation were defined as the beginning and end of the time window, respectively. The time window of the first pass in the myocardial segments at the same level as the LV cavity was determined by shifting the time window determined from the LV cavity by a delay when the SI in the myocardium started to rise, approximately 5 s after contrast arrival to the LV cavity. This method was applied to each slice. The perfusion index (maximal upslope; Upslope) was computed from the peak value of the time derivates of the fit function in the myocardial, normalized by the maximal upslope in the LV cavity. The ratio index, widely acceptable to represent MPR, was defined as the ratio of Upslope at stress to that at rest. All the analyses were performed using in-house software (Mathematica, Wolfram Research, Inc, Champaign, Illinois, USA).

The Upslope at rest and stress and Upslope ratio were computed segment by segment. Each segment was assigned to one of the three corresponding coronary artery territories, i.e., the left anterior descending (LAD), right coronary artery (RCA), and left circumflex coronary artery (LCX) according to the conventional division (17). The myocardial segments were assigned to ischemic segments if the supplying coronary artery showed significant stenosis on coronary angiography; the segments were assigned to remote segments if the supplying arteries were patent (<75% stenosis). All segments in control subjects were considered normal.

Image quality evaluation

We evaluated the image quality of the first-pass enhancement in 8 volunteers randomly chosen from the control group. In each data set, we measured first-pass signal time curves in the

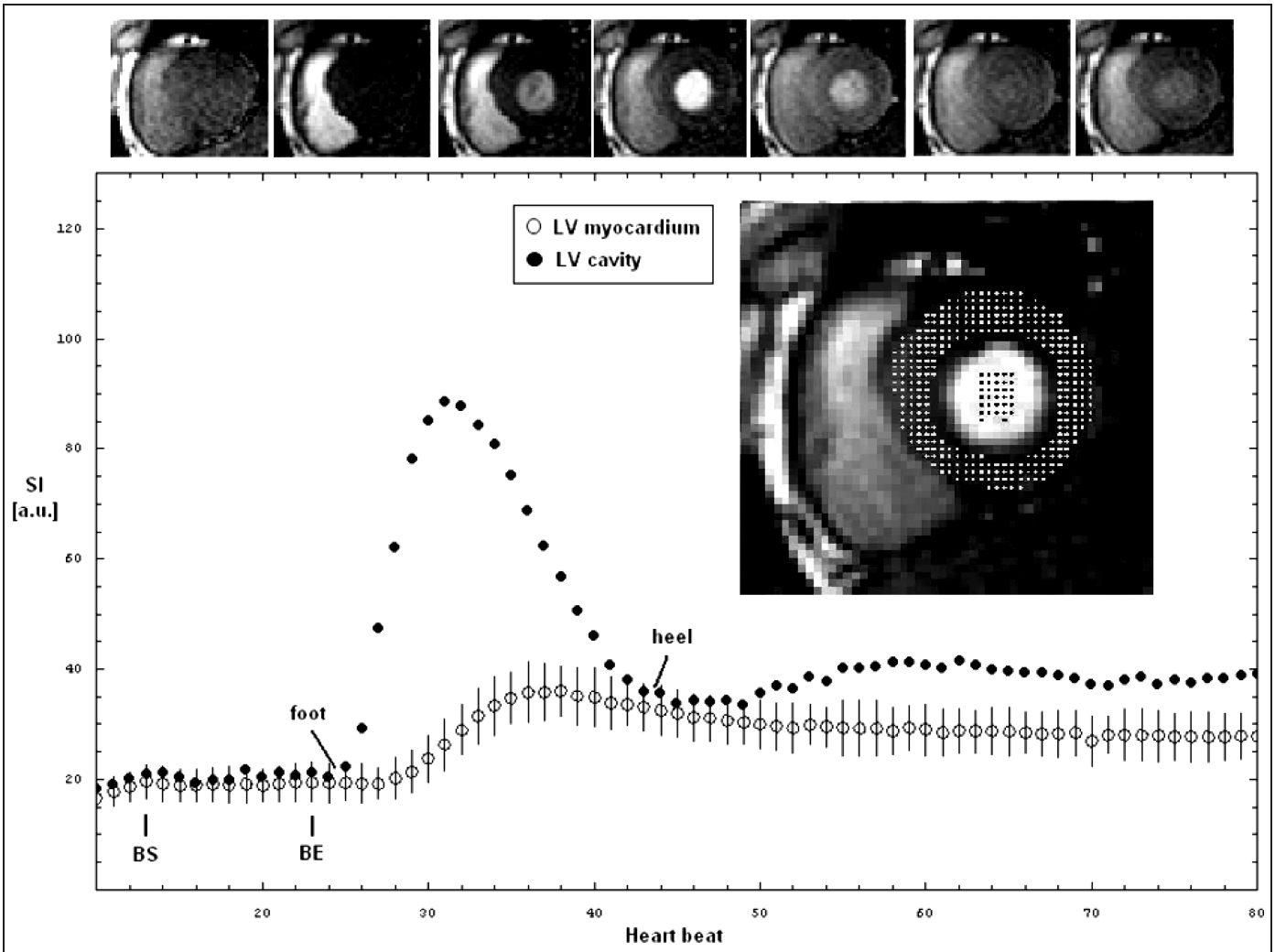

Figure 1. Short axis view of perfusion images derived from SR-turbo FLASH at 3T (top row). Signal intensity (SI) curves of the LV cavity (closed circles) and of the myocardium (open circles) in a normal subject. Each data point in the SI curves represents the mean SI in the LV myocardium and LV cavity at the same short-axis slice (see the inset). The bar represents the standard deviation of the mean. The time window of the first pass is defined from the onset of contrast arrival (foot) to the time before recirculation begins (heel). This time window can be readily identified from the SI curve of the LV cavity, and so it is used to determine the time window in the myocardial SI curve. The baseline SI is determined by averaging SI from base start (BS) to base end (BE).

LV myocardium, and from which we computed CE, SNR and CNR. These quantities in rest and stress states were computed and compared.

Reproducibility

To evaluate the variability of Upslope measurement, intra-observer variability was studied in 8 control subjects and 4 patients randomly chosen from the study subjects. Two measurements were performed by the same operator (SMY) about 6 months apart. The variability was analyzed using Bland-Altman plots (20).

Statistical analysis

The vasodilatation response after dipyridamole infusion was tested by Wilcoxon matched pairs test. Group differences in MPR were tested by Kruskal-Wallis ANOVA test, and Dunn's multiple comparison t-test was used to compare all pairs of groups. Statistical significance was considered if $p < 0.05$.

RESULTS

First-pass perfusion studies in rest and stress states were performed in all subjects without severe side effects. Most participants showed significant increase in the heart rate after the infusion of dipyridamole, resulting in significant increase in the rate pressure product (Table 2). Two normal subjects showed blunted heart rate change (<10 bmp) in the stress test. They were considered to be non-responders and were excluded from the study.

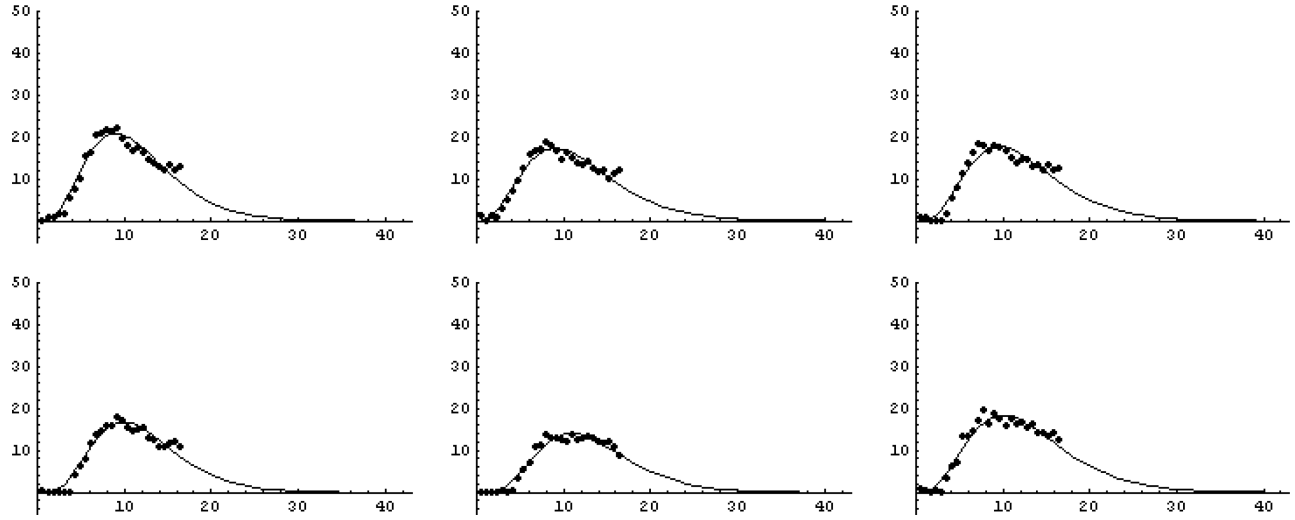

Figure 2. Gamma-variate function was used to smooth-fit the correct SI data within the time window of the first pass in each myocardial segment.

Optimization of contrast medium dose

For the protocol of fixed injection time (N = 6), CE, SNR and CNR in the LV myocardium increased linearly with CM dose over the whole range of dosage (Fig. 3, right). The same parameters in the LV cavity increased linearly up to 0.05 mmol/kg body weight, and showed saturation or a tendency of attenuation from 0.05 to 0.10 mmol/kg body weight (Fig. 3, left).

Coronary angiography

From coronary angiography, 6 out of 12 patients were found to have significant coronary artery stenosis in 10 vessels: 4 were LAD, 3 were RCA and 3 were LCX (Table 1). The other 6 patients showed no significant stenosis in their coronary angiography.

Myocardial perfusion CMR

Normal values of Upslope at rest and stress and Upslope ratios in different coronary territories are listed in Table 3. Averaged Upslope ratios at different segments are shown in Fig. 4. Upslope and Upslope ratio in normal myocardium showed no significant difference among different coronary territories or different segments at each level (p = ns). In the ischemic segments, there was no significant difference in Upslope between rest and stress states (0.11 ± 0.03 vs. 0.10 ± 0.04, p = ns), whereas significant increase was found in the remote (0.09 ± 0.03 vs. 0.13 ± 0.03, $p < 0.001$) and normal segments (0.09 ± 0.03 vs. 0.16 ± 0.05, $p < 0.001$; Fig. 5, left). Upslope ratio in ischemic segments was significantly lower than remote (0.96 ± 0.41 vs. 1.59 ± 0.40, $p < 0.001$) and normal segments (0.96 ± 0.41 vs. 1.71 ± 0.42, $p < 0.001$; Fig. 5, right), but there was no significant difference between remote and normal segments (p = ns). Bull's eye views of color-coded Upslope and MPR of a patient with LAD stenosis is shown in Fig. 6.

Myocardial viability CMR

All control subjects and patients revealed no enhancement in the LGE study.

Image quality

The CE, SNR and CNR derived from myocardium were listed in Table 4. The difference between rest and stress was significant in CE (15.78 ± 5.31 vs. 19.74 ± 6.18, $p < 0.05$) and SNR (17.86 ± 3.24 vs. 23.39 ± 5.78, $p < 0.05$) but not significant in CNR (48.69 ± 20.56 vs. 50.41 ± 19.93, p = ns).

Table 2. Hemodynamic data of control subjects (N = 30)

	Rest	Stress
Heart rate (bpm)	68 ± 7	90 ± 10*
Systolic blood pressure (mm Hg)	119 ± 16	113 ± 17
Diastolic blood pressure (mm Hg)	74 ± 11	71 ± 10
Pulse pressure product (mm Hg*bpm)	8082 ± 1551	10232 ± 2099*

Values are mean±SD.
*Significant difference between rest and stress ($p < 0.05$)

Table 3. Normative perfusion indices (N = 30)

Upslope	LAD	RCA	LCX
rest	0.10 ± 0.03	0.09 ± 0.02	0.09 ± 0.03
stress	0.16 ± 0.06	0.14 ± 0.04	0.16 ± 0.06
ratio	1.62 ± 0.40	1.69 ± 0.39	1.76 ± 0.50

LAD = left anterior descending artery, RCA = right coronary artery, and LCX = left circumflex coronary artery. The indices are listed as mean ± SD

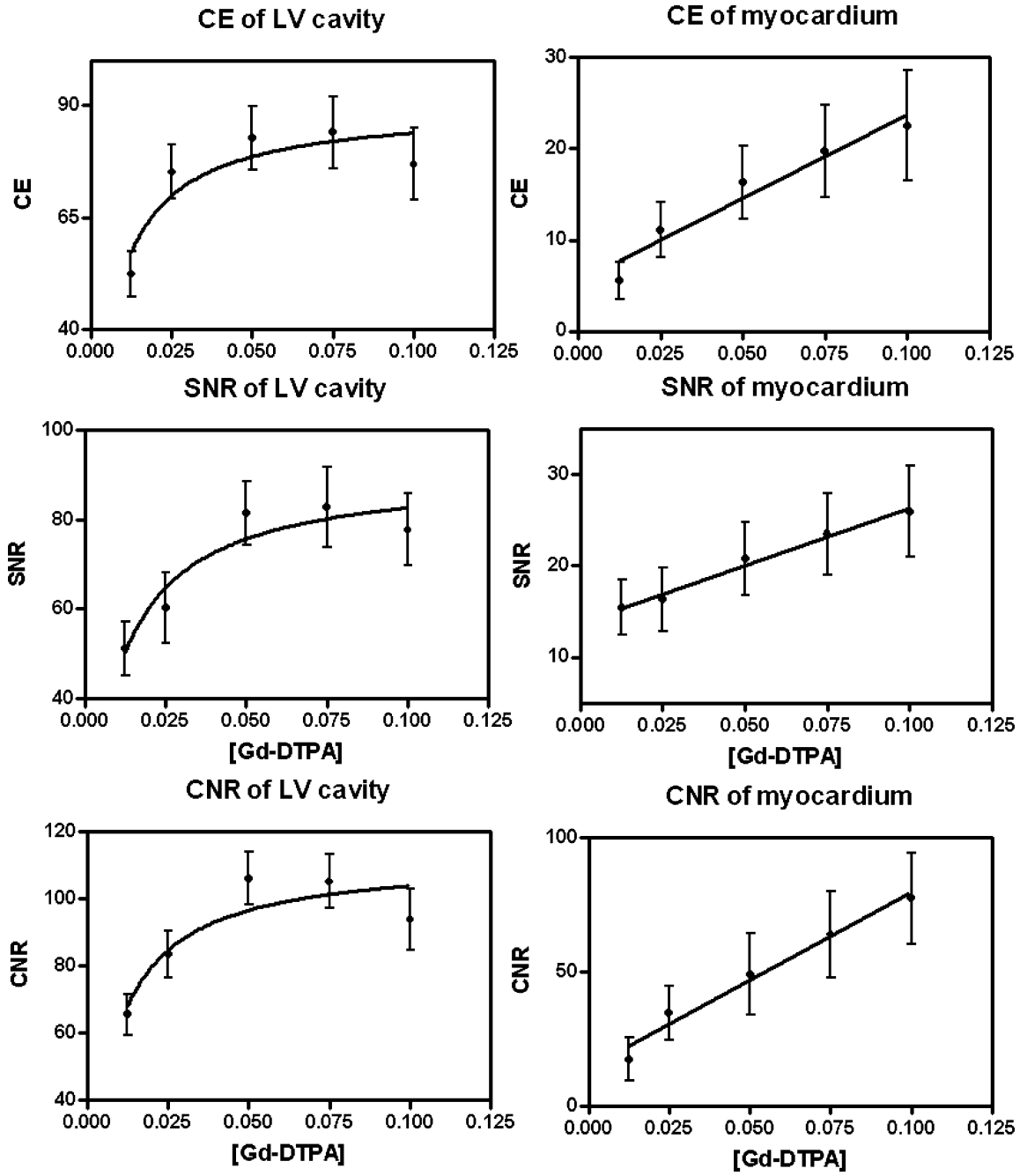

Figure 3. CE, SNR and CNR as a function of Gd-DTPA dose in the LV cavity (left) and myocardium (right). CE, SNR and CNR in the myocardium is linear with contrast dose from 0.0125 to 0.1 mmol/kg body weight, whereas, these parameters in the LV cavity are linear from 0.0125 to 0.05 mmol/kg body weight but becomes saturated in higher doses.

Reproducibility

For the intra-observer variance, the Upslope of repeated measurement ranged from 0.03 to 0.27 with the medium of 0.13. The 95% confidence interval of absolute difference between two repeated measurements of Upslope ranged from −0.007 to 0.008 (Fig. 7).

DISCUSSIONS

CMR at 3T is potentially advantageous due to high SNR and CNR (8–10). However, higher susceptibility artifact has hampered its application to clinical setting. In this study, we demonstrated that with standard imaging protocols and semi-quantitative analysis, assessment of myocardial perfusion at

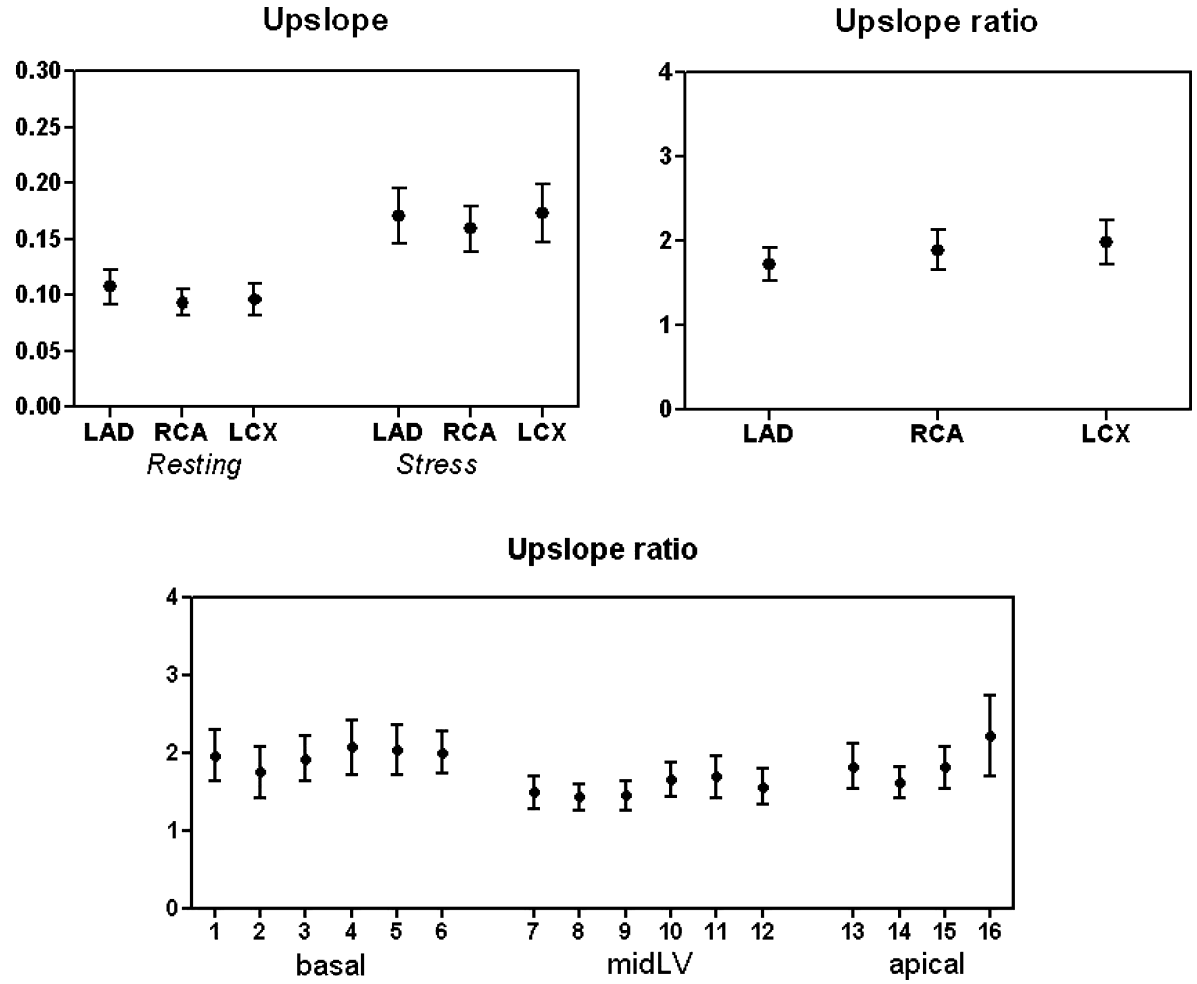

Figure 4. Graphics illustrate the mean ± 95% confidence interval (N = 30) of normative Upslope (top left) and Upslope ratios (top right) in different coronary territories. The Upslope ratio shows no significant difference among 3 coronary territories or among different segments in each level (bottom).

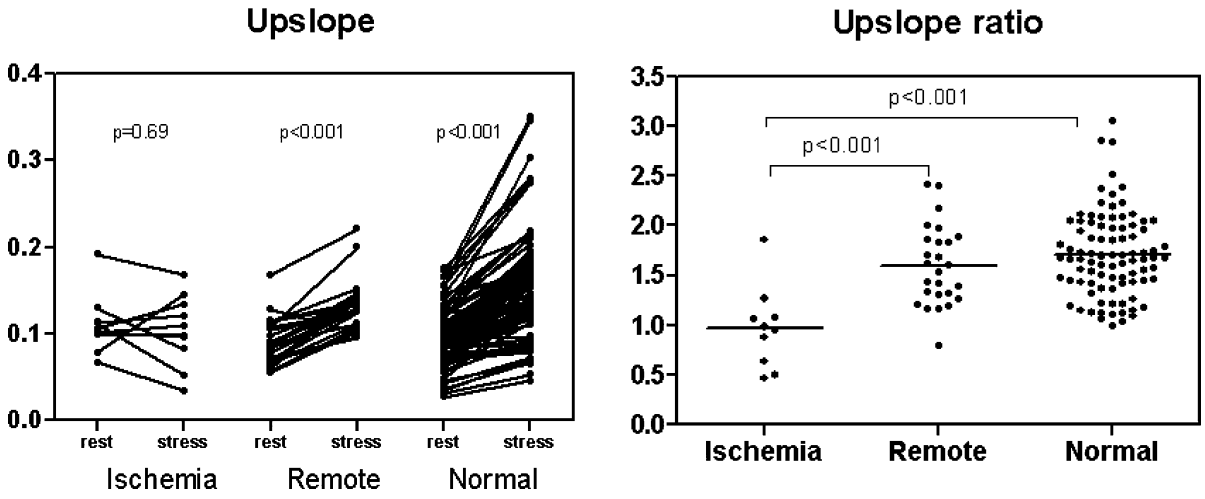

Figure 5. Vasodilatation response of the maximal upslope (Upslope) in the ischemic, remote and normal myocardial segments (left panel). Blunt response of these indices can be seen in the ischemic segments. The ratio indices in the ischemic segments are significantly different from those in the non-ischemic segments (right panel).

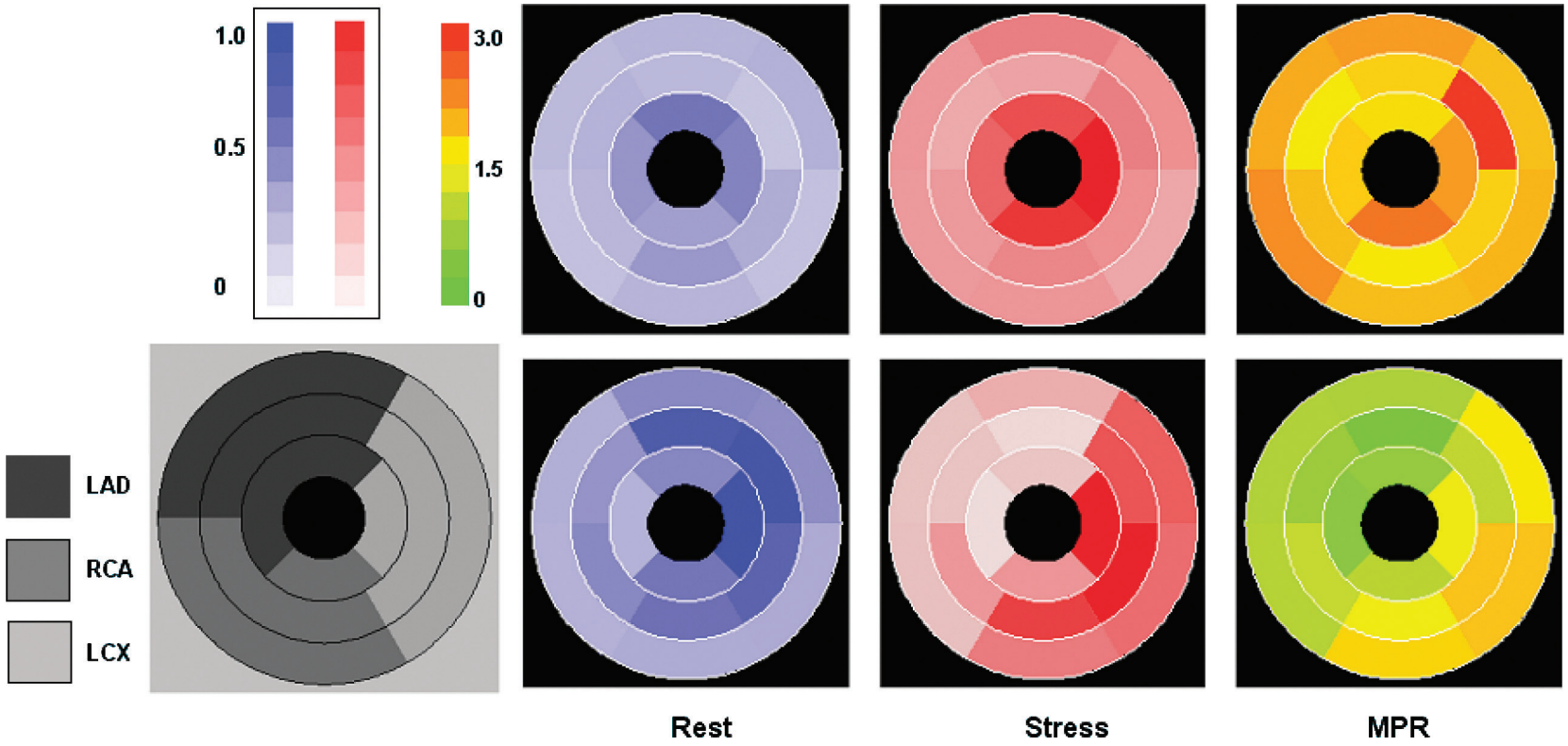

Figure 6. Three short-axis bull's eye views of Upslope at rest, at stress and Upslope ratio (MPR) in a patient with LAD stenosis (bottom row) and a normal subject (upper row). Low MPR can be found in the LAD territory (bottom right), compatible with the distribution map of the coronary artery territories defined by the American Heart Association (bottom left).

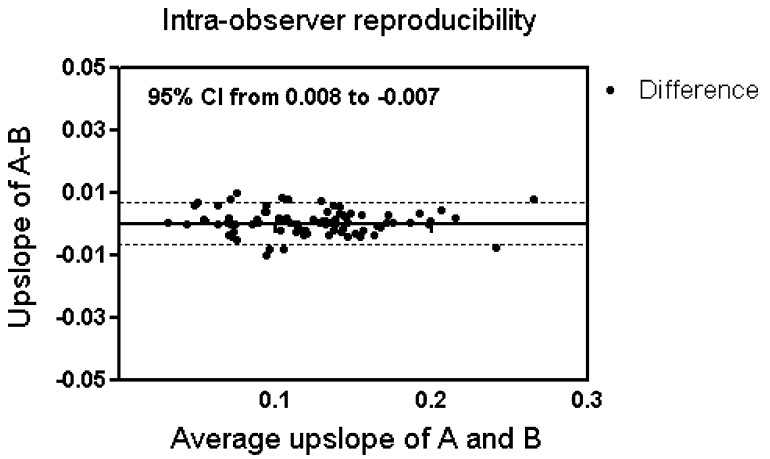

Figure 7. Intra-observer variability of Upslope measurement from 8 normal volunteers and 4 patients randomly chosen from the study subjects. On average, the variability is about 6% of the Upslope.

3T is feasible. From 30 healthy subjects, we obtained normative values of Upslope at rest and stress and Upslope ratio. These values were rather constant across different coronary territories and myocardial segments. In the prospective study of 12 patients, Upslope ratios in the angiographically documented ischemic myocardium were significantly different from the values in the remote and normal myocardium.

In this study, the pulse sequence, SR-prepped TurboFLASH, is a standard "ready to use" sequence, which is the same as the sequence used at 1.5T. In our center, we have performed CMR study at 1.5T and 3T. Consistent with the reports from other centers, we found that CMR at 3T, with optimum setting of the scanning parameters, shows higher SNR, better perfusion contrast and delayed enhancement (9–10, 21). Owing to longer T1 relaxation time and higher specific absorption rate (SAR) at 3T, parameters such as TI, TR and flip angle have been adjusted. It is also known that magnetic susceptibility-induced artifact increases with the magnetic field. Therefore, adjustment of the center frequency shift and shimming of the magnetic field are performed routinely at the beginning of each CMR study.

Myocardial perfusion can be assessed with CMR using visual detection, quantitative (4, 23–25) or semi-quantitative analysis (5–7, 26–32). Visual detection can be made on site without delaying the reporting. However, only limited data are available regarding the accuracy of visual assessment (33). This is due in part to the fact that the diagnostic accuracy relies heavily on the experience of the observer. Susceptibility artifact and inhomogeneous signal distribution will potentially cause confusion in the interpretation. These potential pitfalls become more significant at 3T. In contrast, quantitative or semi-quantitative analysis is less observer-dependent and can avoid the confounding effects mentioned above. Quantitative analysis invokes pharmacokinetic models in which tracer exchange between the LV blood pool and the myocardium is modeled mathematically. The parameters derived from such model-based approach have direct physiological implication. Semi-quantitative analysis characterizes SI curves in terms of maximal upslope, peak value, time to peak or area under the curve. Although these parameters provide little physiological meaning, human and animal studies have demonstrated that they reflect MPR with high reproducibility and accuracy (3, 5, 26). Currently, both quantitative and semi-quantitative methods are time-consuming, and their accuracy is dependent on operators and algorithms. Further progress in automation of the algorithm and reduction of computation time is needed to implement these methods in the clinical setting.

Table 4. Data evaluation: CE, SNR and CNR (N = 8)

	CE		SNR		CNR	
	Rest	Stress	Rest	Stress	Rest	Stress
Mean	15.78	19.74	17.86	23.39	48.69	50.41
STD	5.31	6.18	3.24	5.78	20.56	19.93
Significance: pair *t* test	$p < 0.05$		$p < 0.05$		NS	

In quantitative or semi-quantitative analysis, adequate perfusion contrast and linearity between CM dose and SI must be ensured for reliable tracer kinetic analysis. In 1.5T MR systems, the optimum dose has been investigated (4–7, 22–32), but at 3T, it is still unknown. In our study, CE, SNR and CNR in the myocardium increases linearly with CM dose. However, in the LV cavity the linearity breaks down if CM dose exceeded 0.05 mmol/kg body weight. This can be understood by the fact that high concentration of CM causes longer time for full magnetization and shorter T2* (34). In order to maintain adequate perfusion contrast in the myocardium and to keep SI linearity in the myocardium and LV cavity, 0.025 mmole/kg body weight appears to be the optimum dose with the given sequence and mode of analysis in this study. Gutberlet et al (10) compared the image quality of myocardial perfusion imaging at rest between 1.5T and 3T. They reported that 3T offered significant improvement in SNR and CNR than 1.5T, and there was no significant difference in susceptibility artifact between two fields. In our

study, 0.025 mmol/kg body weight CM dose was used, which was a half of what they used. Contrast-induced susceptibility artifact was not found either. Additionally, our SNR at rest was still comparable with their results, 17.86 ± 3.24 vs. 13.2 ± 3.5.

The dose optimization study was originally performed on one subject by fixing the injection rate at 4 mL/s. With this protocol, we found that higher dose lead to longer bolus duration and made the time course of the first pass broader. The variation in the time course of the first pass at different doses will inevitably affect the result of upslope calculation, which is not physiological. If we fixed the injection time to ensure that different CM doses could be administered within the same time interval, the upslope calculated at different doses were more stable. Therefore, we decided to use the protocol of fixed injection time rather than fixed injection rate. Although, our results were obtained from a small size of samples ($N = 6$), the linearity behavior in each subject appeared quite consistent with each other.

From the coronary angiography of our 12 patients, 6 patients had hemodynamically-significant stenosis (>75%) in ten coronary arteries (Table 1). Among them, 4 patients had severe stenosis (>95%) in 4 coronary arteries. Only 2 patients with severe stenosis at proximal segments showed visually-detectable perfusion defects in perfusion CMR (Fig. 6). For the rest of the coronary lesions, showing either severe stenosis at distal segment or moderate stenosis at either proximal or distal segment in angiography, all of them did not show visually-detectable perfusion defects. Most of these lesions, however, were differentiable from the normal myocardium based on the measurement of Upslope ratio. Therefore, the dose of 0.025 mmol/kg body weight used in this study is optimum for quantitative or semi-quantitative analysis but may be inadequate for visual detection of perfusion defect. In our volunteers, no visual perfusion defect was observed.

In this paper, we found that Upslope and Upslope ratio were rather constant among different coronary territories and different myocardial segments in normal volunteers. These findings are consistent with a previous report at 1.5T by Plein et al (35). In Figure 5, we showed that Upslope ratio could distinguish the ischemic and remote myocardium. Typically, Upslope decreased from rest to stress in the ischemic segments and increased in the remote myocardium. However, there were one ischemic segment and one remote segment showing opposite tendency. The reasons for the mismatch might be due to, respectively, development of collateral circulation and stenosis involving the small vessels (4, 36). Collateral circulation secondary to epicardial stenosis may have normal response to vasodilator and manifests normal Upslope ratio in the supplied myocardium. In contrast, small vessel narrowing may be detected by perfusion CMR but is likely to be missed by coronary angiography due to poor detection of stenosis in small vessels.

One of the goals in the first-pass gadolinium-enhanced CMR is to assess myocardial perfusion at different wall depths. Mapping out transmural perfusion gradient is more sensitive to detect subendocardial ischemia than measuring average perfusion across the wall. Transmural difference of myocardial blood flow under normal conditions has been reported previously (37). This difference accentuates if epicardial coronary arteries narrow and can serve as a marker to predict the severity of coronary artery stenosis (38, 39). Panting et al (31) reported that in patients with syndrome X, perfusion CMR revealed subendocardial hypoperfusion during stress test. Other studies also showed that subendocardial perfusion impairment might be useful to indicate early ischemia, particularly in "hibernating" or "stunned" myocardium (40). Several study groups have demonstrated that first-pass myocardial perfusion CMR with pixel size less than 3 mm is sufficient to differentiate subendocardial from subepicardial perfusion (29).

Taking the advantage of higher SNR and perfusion contrast at 3T, we performed pixel-based semi-quantitative analysis on a patient with three-vessel disease who had subendocardial infarction in the anterior segment and interventricular septum. Relatively low Upslope is detected in the color-coded Upslope map, corresponding to the hyperenhanced regions shown in the LGE study (Fig. 8).

In conclusion, 0.025 mmole/kg body weight is the optimum dose for perfusion study at 3T with given sequence and mode

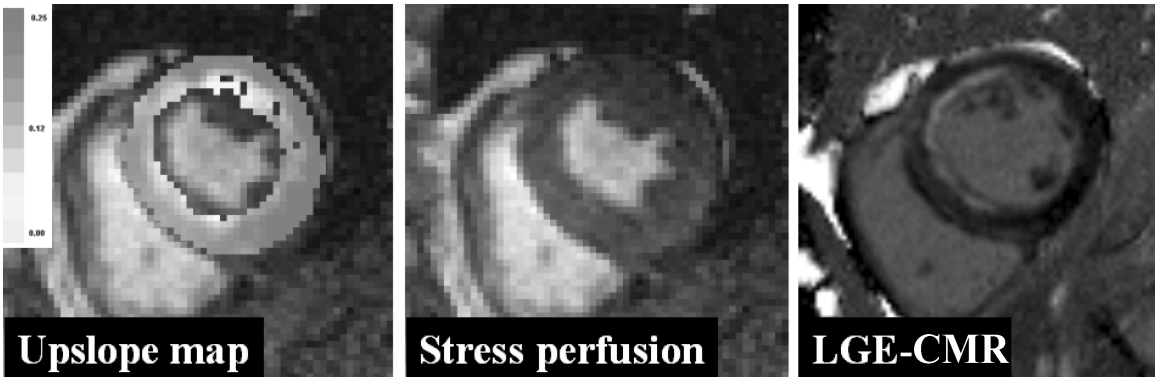

Figure 8. Pixel-based Upslope map (left) at stress shows a subendocardial perfusion defect, corresponding to the subendocardial hyperenhancement shown on the late gadolinium-enhanced (LGE) CMR (right). In this case, it is difficult to visualize the perfusion defect on the image of stress perfusion (middle).

of analysis in this study. Using this dosage, adequate perfusion contrast can be obtained with reproducible semi-quantitative results and no contrast-induced susceptibility artifact. Upslope and Upslope ratio can differentiate ischemic from non-ischemic myocardium. Therefore, first-pass gadolinium-enhanced myocardial perfusion imaging is feasible at 3T.

REFERENCES

1. Atkinson DJ, Burstein D, Edelman RR. First-pass cardiac perfusion: evaluation with ultrafast MR imaging. Radiology 1990;174:757–762.
2. Gould KL, Lipscomb K. Effects of coronary stenosis on coronary flow reserve and resistance. Am J Cardiol 1974;34:48–55.
3. Wilke N, Jerosch-Herold M, Wang Y, et al. Myocardial perfusion reserve: assessment with multisection, quantitative, first-pass MR imaging. Radiology 1997;204:373–384.
4. Cullen JHS, Horsfield MA, Reek CR, et al. A myocardial perfusion reserve index in humans using first-pass contrast-enhanced magnetic resonance imaging. J Am Coll Cardiol 1999;33:1386–1394.
5. Al-Saadi N, Nagel E, Gross M, et al. Noninvasive detection of myocardial ischemia from perfusion reserve based on cardiovascular magnetic resonance. Circulation 2000;101:1379–1383.
6. Al-Saadi N, Gross M, Paetsch I, et al. Dobutamine induced myocardial perfusion reserve index with cardiovascular MR in patients with coronary artery disease. J Cardiovasc Magn Reson 2002;4:471–480.
7. Nagel E, Klein C, Paetsch I, et al. Magnetic resonance perfusion measurements for the noninvasive detection of coronary artery disease. Circulation 2003;108:432–437.
8. Nayak KS, Cunningham CH, Santos JM, et al. Real-time cardiac MRI at 3 tesla. Magn Reson Med 2004;51:655–60.
9. Araoz PA, Glockner JF, McGee KP, et al. 3 Tesla MR imaging provides contrast in first-pass myocardial perfusion imaging over a range of gadolinium doses. J Cardiovasc Magn Reson 2005;7:559–64.
10. Gutberlet M, Noeske R, Schwingo K, et al. Comprehensive cardiac magnetic resonance imaging at 3.0Tesla: Feasibility and Implications for clinical applications. Invest Radiol 2006;41:154–167.
11. Atalay MK, Poncelet BP, Kantor HL, et al. Cardiac susceptibility artifacts arising from the heart-lung interface. Magn Reson Med 2001;45:341–345.
12. Al-Saadi N, Nagel E, Gross M, et al. Improvement of myocardial perfusion reserve early after coronary intervention: assessment with cardiac magnetic resonance imaging. J Am Coll Cardiol 2000;36:1557–1564.
13. Fenchel M, Helber U, Simonetti OP, et al. Multislice first-pass myocardial perfusion imaging: Comparison of saturation recovery (SR)-TrueFISP-two-dimensional (2D) and SR-TurboFLASH-2D pulse sequences. JMRI 2004;19:555–563.
14. Jerosch-Herold M, Seethamraju RT, Swingen CM, et al. Analysis of myocardial perfusion MRI. J Magn Reson Imaging 2004;19:758–770.
15. Ryan TJ, Faxon DP, Gunnar RM, et al. Guidelines for percutaneous transluminal coronary angioplasty. Circulation, 1998;78:486–502.
16. Vallee JP, Sostman HD, MacFall JR, et al. MRI quantitative myocardial perfusion with compartmental analysis: a rest and stress study. Magn Reson Med 1997;8:981–989.
17. Cerqueira MD, Weissman NJ, Dislsizian V, et al. Standardized myocardial segmentation and nomenclature for tomographic imaging of the heart: a statement for healthcare professionals from the Cardiac Imaging Committee of the Council on Clinical Cardiology of the American Heart Association. Circulation 2002;105:539–542.
18. Thompson HK, Starmer CF, Whalen RE, et al. Indicator transit time considered as a gamma variate. Circ Res 1964;14:502–515.
19. Keijer JT, Rossum ACV, Eenige MJV, et al. Semiquantitation of regional myocardial blood flow in normal human subjects by first-pass magnetic resonance imaging. Am Heart J 1995;130:893–901.
20. Dewitte K, Fierens C, Stockl D. Application of the Bland-Altman plot for interpretation of method comparison studies: A critical investigation of its practice. Clinical Chemistry 2002;48:799–801.
21. Sandman DN, Salantri J, Simonetti O, et al. First-pass resting myocardial perfusion at 3T. *ISMRM 14th Scientific Meeting and Exhibition,* Miami, FL, USA, p255.
22. Matheijssen NA, Louwerenburg HW, Rugge FP, et al. Comparison of ultrafast dipyridamole magnetic resonance imaging with dipyridamole SestaMIBI SPECT for detection of perfusion abnormalities in patients with one-vessel coronary artery disease: assessment by quantitative model fitting. Magn Reson Med 1996;35:221–228.
23. Jerosch-Herold M, Wilke N, Stillman AE, et al. MR quantification of the myocardial perfusion reserve with a Fermi function model for constrained deconvolution. Med Phys 1998;25:73–84.
24. Vallee JP, Lazeyras F, Kasuboski L, et al. Quantification of myocardial perfusion with FAST sequence and Gd bolus in patients with normal cardiac function. JMRI 1999;9:197–203.
25. Neyran B, Janier MF, Casali C, et al. Mapping myocardial perfusion with an intravascular MR contrast agent: robustness of deconvolution methods at various blood flows. Magn Reson Med 2002;48:166–179.
26. Wilke N, Simm C, Zhang J, et al. Contrast-enhanced first pass myocardial perfusion imaging: correlation between myocardial blood flow in dogs at rest and during hyperemia. Magn Reson Med 1993;29:485–497.
27. Kraitchman DL, Wilke N, Hexeberg E, et al. Myocardial perfusion and function in dogs with moderate coronary stenosis. Magn Reson Med 1996;35:771–780.
28. Kirsi L, Kari SV, Leena MS, et al. Multislice MRI in assessment of myocardial perfusion in patients with single-vessel proximal left anterior descending coronary artery disease before and after revasculation. Circulation1997;96:2859–2867.
29. Wilke N, Jerosch-Herold M, Zenovich A, et al. Magnetic resonance first-pass myocardial perfusion imaging: clinical validation and future applications. JMRI 1999;10:676–685.
30. Klocke FJ, Simonetti OP, Judd RM, et al. Limits of detection of regional differences in vasodilated flow in viable myocardium by first-pass magnetic resonance perfusion imaging. Circulation 2001;104:2412–2416.
31. Panting JR, Gatehouse PD, Yang GZ, et al. Abnormal subendocardial perfusion in cardiac syndrome X detected by cardiovascular magnetic resonance imaging. N Engl J Med 2002;346:1948–1953.
32. Jerosch-Herold M, Hu X, Murthy NS, et al. Magnetic resonance imaging of myocardial contrast enhancement with MS-325 and its relation to myocardial blood flow and the perfusion reserve. JMRI 2003;18:544–554.
33. Ishida N, Sakuma H, Motoyasu M, et al. Noninfarcted Myocardium: Correlation between Dynamic First-Pass Contrast-enhanced Myocardial MR Imaging and Quantitative Coronary Angiography. Radiology 2003;229:209–216.
34. Neimatallah MA, Chenevert TL, Carlos RC, et al. Subclavian MR arteriography: reduction of susceptibility artifact with short echo time and dilute gadopentetate dimeglumine. Radiology 2000;217:581–586.
35. Plein S, Radjenovic A, Ridgway JP. Coronary artery disease: myocardial perfusion MR imaging with sensitivity encoding versus conventional angiography. Radiology 2005;235:423–430.
36. Wolff SD, Schwitter J, Coulden R, et al. Myocardial first-pass magnetic resonance imaging: A multicenter dose-ranging study. Circulation 2004;110:732–737.

37. Path G, Robitaille PM, Merkle H, et al. Correlation between transmural high energy phosphate levels and myocardial blood flow in the presence of graded coronary stenosis. Circ Res 1990;67:660–673.

38. Lee DC, Simonetti OP, Harris KR, et al. Magnetic resonance versus radionuclide pharmacological stress perfusion imaging for flow-limiting stenosis of varying severity. Circulation 2004;110:58–65.

39. Keijer JT, vanRossum AC, Wilke N, et al. Magnetic resonance imaging of myocardial perfusion in single-vessel coronary artery disease: Implications for transmural assessment of myocardial perfusion. J Cardiovasc Magn Reson 2000;2:189–200.

40. Fallavollita AJ, Perry BJ, Canty MJ. 18F-2-Deoxyglucose deposition and regional flow in pigs with chronically dysfunctional myocardium. Circulation 1997;95:1900–1909.